J. Astrophys. Astr. (2019) 40:44
https://doi.org/10.1007/s12036-019-9613-2

Reconstruction of dynamical dark energy potentials: Quintessence, tachyon and interacting models

MANVENDRA PRATAP RAJVANSHI* and J. S. BAGLA

Indian Institute of Science Education and Research Mohali, Knowledge City, Sector 81, Sahibzada Ajit Singh Nagar, Punjab 140 306, India.
*Corresponding author.
E-mail: manvendra@iisermohali.ac.in; jasjeet@iisermohali.ac.in

MS received 21 May 2019; accepted 7 October 2019

Abstract. Dynamical models for dark energy are an alternative to the cosmological constant. It is important to investigate properties of perturbations in these models and go beyond the smooth FRLW cosmology. This allows us to distinguish different dark energy models with the same expansion history. For this, one often needs the potential for a particular expansion history. We study how such potentials can be reconstructed by obtaining closed formulae for potential or reducing the problem to quadrature. We consider three classes of models here: tachyons, quintessence and interacting dark energy. We present results for the constant w and the CPL parametrization. The method given here can be generalized to any arbitrary form of $w(z)$.

Keywords. Cosmology: dark energy—theory.

1. Introduction

Observations (Riess *et al.* 1998; Perlmutter *et al.* 1999) have indicated that the Universe is expanding at an increasing rate. This has led to dark energy (Efstathiou *et al.* 1990; Ostriker & Steinhardt 1995; Bagla *et al.* 1996; Amendola & Tsujikawa 2010), the component with unusual properties that causes the accelerated expansion of the Universe. Besides the simple and successful cosmological constant model (Λ), there are a number of competing theories (Amendola & Tsujikawa 2010; Durrer 2011; Bamba *et al.* 2012) that are consistent with observations. In these theories, dark energy is dynamical in that its properties are a function of space and time. In order to study the theoretical and observational implications for these theories, we have to solve the equations describing the dark energy. Analysis of some observations only requires the variation of scale factor with time, however, other observations can have a dependence on spatial variations in dark energy and thus details of the model become relevant.

A number of models have been proposed for dark energy, e.g., tachyon dark energy (Padmanabhan 2002; Bagla *et al.* 2003) and quintessence (Tsujikawa 2013; Caldwell *et al.* 1998). In both of these, a scalar field and its gradients give rise to dark energy densities, but the forms of the Lagrangian densities for these are very different.

It is well known that if two models have the same evolution of the scale factor, tests relying only on distance measurements cannot distinguish between such models. Therefore, it is important to study growth of perturbations in matter for different models of dark energy with the same evolution of the scale factor. This opens up comparison based on CMB anisotropies (Jassal 2012; Wang *et al.* 2010; Mifsud & Van De Bruck 2017), weak lensing (De Bernardis *et al.* 2011; Pettorino & Baccigalupi 2008; Yang *et al.* 2016) and growth of perturbations (Rajvanshi & Bagla 2018). In this context, it is useful to have a formalism for constructing potentials for different models of dark energy that lead to the same expansion history. In this article, we compute the corresponding potentials in quintessence and tachyon models which can give the same background evolution. We reconstruct potential $V(\phi)$ assuming a particular equation of state $w(z)$. We give analytical expressions wherever possible, in other cases we reduce the problem to quadrature for numerical reconstruction of $V(\phi)$.

There has been a lot of interest in recovering dark energy potential from the observed expansion history

Published online: 28 November 2019

(Wu & Yu 2007; Sahni & Starobinsky 2006; Saini *et al.* 2000). For example, Huterer and Turner (1999) provided an early work on constructing potential from simulated data and inspired further research. Li *et al.* (2007) constructed a potential by approximating luminosity distances and also did a comparison for reconstruction using parametrization of equation of state $w(z)$. A number of other attempts for reconstruction using a parametric or a non-parametric approach have been made (for example, see Gerke & Efstathiou 2002; Clarkson & Zunckel 2010; Huterer & Shafer 2018 for a review). We approach this problem by attempting to construct a potential for a given redshift dependence of the equation of state parameter $w(z)$ for the dark energy component. We do this for both quintessence and tachyon models. While a number of solutions exist for quintessence models (Scherrer 2015; Battye & Pace 2016), few solutions are available for tachyon models. In Scherrer (2015), a mapping between CPL parameters and potentials is explored while an analytic approximation for various scalar field models is obtained by Battye and Pace (2016).

In Section 2, we set up equations for tachyon and quintessence models. In Sections 2.2 and 2.3, we do reconstruction of a potential for $w(z) =$ constant. In Section 3, we outline the numerical recipe for reconstruction for any general $w(z)$ and illustrate it with results for some simple cases.

2. Basic equations

We are interested in late time evolution of the Universe. Given the observations that indicate that the spatial curvature is consistent with zero, and that radiation does not contribute to the expansion history at $z \leq 100$, we choose to work with only matter and dark energy. The method we outline can be generalized without any modifications to include other cases. For illustration of the method, we work with the CPL parametrization (Chevallier & Polarski 2001; Linder 2003). The functional form for $w(z)$ is defined in terms of two constants, which we call p and q:

$$w = p + q(a - a_i), \tag{1}$$

where p is the value of w at some $t = t_i$ while q gives the rate of change of w with the scale factor. Symbols w_0 (for p) and w_1 (for q) are often used while using this parametrization, if t_i is taken to be the present time t_0. Continuity equation for dark energy density $\rho_{\rm de}$ is

$$\frac{{\rm d}\rho_{\rm de}}{{\rm d}t} = -3(1 + p + q(a - a_i))\frac{\dot{a}}{a}\rho_{\rm de}. \tag{2}$$

Using this equation, we get

$$\rho_{\rm de} = \rho^i_{\rm de}\left(\frac{a_i}{a}\right)^{3(1+p-qa_i)} \exp[-3q(a - a_i)], \tag{3}$$

where $\rho^i_{\rm de}$ is the density at some initial time. From now on, we use a scaled dimensionless variable for time $t = tH_i$. Friedmann equation then takes the form

$$\frac{\dot{a}^2}{a^2} = \frac{\alpha}{a^3} + \frac{\beta}{a^{3(1+p-qa_i)}e^{3qa}}, \tag{4}$$

where α and β are constants defined as

$$\alpha = \Omega_{m\,i}, \quad \beta = (1 - \Omega_{m\,i})a_i^{3(1+p-qa_i)}{\rm e}^{3qa_i}. \tag{5}$$

These are related to the density parameter for matter and dark energy at the initial time.

2.1 *Tachyon field*

Tachyon models for dark energy have an action of the following form:

$$I = \int d^4x\sqrt{-g}\big[-V(\phi)\sqrt{1 - \partial^\mu\phi\partial_\mu\phi}\big]. \tag{6}$$

In these models, the energy density and pressure can be written as

$$\rho_\phi = \frac{V(\phi)}{\sqrt{1 - \partial^\mu\phi\partial_\mu\phi}},$$
$$P_\phi = -V(\phi)\sqrt{1 - \partial^\mu\phi\partial_\mu\phi}.$$

For these models, the equation of state parameter is related to the time derivative of the field as $w = -1+\dot{\phi}^2$ for a homogeneous field. Thus we have

$$\frac{{\rm d}\phi}{{\rm d}t} = \sqrt{1 + p + q(a - a_i)}. \tag{7}$$

Combining Equations (4) and (7), we have

$$\phi(a) = \int \frac{\sqrt{a(1 + p + q(a - a_i))}}{\sqrt{\alpha + \frac{\beta}{a^{3p-qa_i}\,{\rm e}^{3qa}}}}{\rm d}a. \tag{8}$$

Using the relation between the energy density and the potential, we can write

$$V(\phi) = \sqrt{-w}\rho_{\rm de}. \tag{9}$$

Since we know $\rho_{\rm de}$ as a function of a, from Equation (3), we can compute $V(a)$. The combination of Equations (8) and (9) gives a parametric solution for the potential as a function of the field ϕ, with the scale factor a playing the role of the intermediate parameter.

2.2 *Tachyon field: Constant w*

We start by considering the special case of $w =$ constant, i.e., $q = 0$. The integral in Equation (8) takes the

following form for constant w:

$$\phi(a) = \int \frac{\sqrt{a(1+w)}}{\sqrt{\alpha + \frac{\beta}{a^{3w}}}} \mathrm{d}a. \tag{10}$$

Defining

$$x^2 = \alpha + \frac{\beta}{a^{3w}} \tag{11}$$

reduces the integral to

$$\phi(x) = \int \frac{\sigma}{(x^2-\alpha)^k} \mathrm{d}x, \tag{12}$$

where σ and k are

$$\sigma = -\frac{2\sqrt{1+w}}{3w\beta}\beta^k, \qquad k = \frac{w+\frac{1}{2}}{w}. \tag{13}$$

The integral in Equation (12) is trivial for $w = -\frac{1}{2}$, where we get

$$\phi(a) = \sigma\sqrt{\alpha + \beta a^{3/2}}. \tag{14}$$

The potential $V(a)$ for the constant w is

$$\frac{V(a)}{H_i^2} = \frac{3\sqrt{-w}\beta}{8\pi G a^{3(1+w)}}. \tag{15}$$

When $w = -\frac{1}{2}$, we get

$$\frac{V(\phi)}{H_i^2} = \frac{3\beta}{8\pi G\sqrt{2}\left[\frac{\phi^2}{\beta\sigma^2} - \frac{\alpha}{\beta}\right]}. \tag{16}$$

For other values of w, the integral in Equation (10) does not have a closed form solution. The result can be expressed in the form of hypergeometric functions

$$\begin{aligned}\phi(a) =& \frac{2a}{3}\left[\frac{a(1+w)(\beta a^{-3w}+\alpha)}{\alpha(\beta a^{-3w}+\alpha)}\right]^{1/2} \\ &\times\ {}_2F_1\left[\frac{1}{2}, -\frac{1}{2w}; 1-\frac{1}{2w}; -\frac{a^{-3w}\beta}{\alpha}\right].\end{aligned} \tag{17}$$

From Equation (15), we have $V(a)$, and we need to invert Equation (17) to get $a(\phi)$ and substitute it in Equation (15) to get $V(\phi)$. Please note that for background calculations, one does not really need $V(\phi)$, as $V(a)$ contains the relevant information. However, for a study of spatial perturbations, we require $V(\phi)$ as ϕ can take on different values at different points at a given time. A number of numerical libraries provide routines for calculation of ${}_2F_1(a,b,c,g)$. GNU Scientific Library has function `gsl_sf_hyperg_2F1`, which computes ${}_2F_1(a,b,c,g)$ for $|g| < 1$. In case of Equation (17), $g < 0$ and for extending to $g < -1$, there are standard transformations available in literature (see Pearson's thesis (2009) for a detailed account of computation of hypergeometric functions, we use transformations mentioned in section 4.6 of Pearson's thesis (2009)). For $g = -\frac{a^{-3w}\beta}{\alpha} < -1$, we use following formulae for computing ${}_2F_1(a,b,c,g)$:

$$\begin{aligned}{}_2F_1(a,b,c,g) =& \frac{1}{(1-g)^a}\frac{\Gamma(c)\Gamma(b-a)}{\Gamma(b)\Gamma(c-a)} \\ & {}_2F_1\left(a, c-b, a-b+1, \frac{1}{(1-g)}\right) \\ &+ \frac{1}{(1-g)^b}\frac{\Gamma(c)\Gamma(a-b)}{\Gamma(a)\Gamma(c-b)} \\ & {}_2F_1\left(b, c-a, b-a+1, \frac{1}{(1-g)}\right).\end{aligned} \tag{18}$$

Equation (10) can be written in the form of a differential equation which makes its relationship with other functions clear. Let

$$g = -\frac{a^{-3w}\beta}{\alpha}. \tag{19}$$

Then Equation (10) can be differentiated to obtain

$$g(1-g)\frac{\mathrm{d}^2\phi}{\mathrm{d}g^2} + \left[\left(\frac{1}{2w}+1\right) - \left(\frac{3}{2}+\frac{1}{2w}\right)g\right]\frac{\mathrm{d}\phi}{\mathrm{d}g} = 0. \tag{20}$$

It can be integrated twice to obtain $\phi(g)$ in terms of incomplete beta functions $B(g;a,b)$, which are related to ${}_2F_1(a,b,c,g)$:

$$\phi(g) = C_1 B(g; 1-u, 1+u+v) + C_2, \tag{21}$$

where C_1, C_2 are constants of integration and

$$\begin{aligned}u &= \left(\frac{1}{2w}+1\right), \\ v &= -\left(\frac{3}{2}+\frac{1}{2w}\right).\end{aligned} \tag{22}$$

$B(g;a,b)$ is related to ${}_2F_1(a,b,c,g)$ (Weisstein webpage 2018) as follows:

$$B(g;a,b) = \frac{g^a}{a}{}_2F_1(a, 1-b, a+1, g). \tag{23}$$

We can invert either Equation (17) or Equation (23) to obtain $a(\phi)$ and then use Equation (15) to obtain $V(\phi)$. We have used the Newton–Raphson method for inversion from $\phi(a)$ to $a(\phi)$ and then to $V(\phi)$. This is useful in dynamically calculating $V(\phi)$ and the derivative $V_\phi(\phi)$ when ϕ has spatial variations in the presence of perturbations.

2.2.1 Form of the potential for constant w. Here we plot (Figure 1) the potential $V(\phi)$ for different values

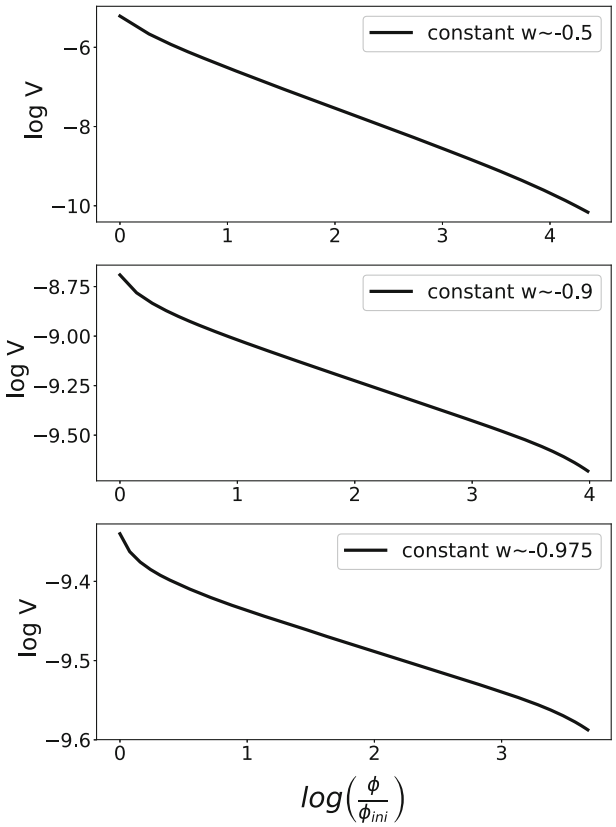

Figure 1. We plot tachyon potentials simulated for constant w, using methods described in the previous section. Different panels are for different constant w values.

of w. We can see from the plot that the dependence of $V(\phi)$ is close to a power law. To get insight into this behaviour, we plot derivatives of log of potential with respect to log of field in Figure 2. We see that in the central part, there is an approximate flat curve indicating that in this region the potential can be approximated by power laws.

We can approximate potential in this flat region with the form

$$V(\phi) = c\phi^b. \tag{24}$$

For this form we have done fitting for different values of constant w and then we find the relationship between constant w and b which is linear as shown in Figure 3. These fittings are crude given that evolution of w and other quantities is very sensitive to form a potential.

This can potentially be used to constrain the potential for tachyon fields if one already has observational constraints on w. We are working on a detailed analysis of observational constraints to be presented in a forthcoming publication. Here we present an example of such an exercise. We make use of the existing studies of observational constrains on wCDM models. In one such

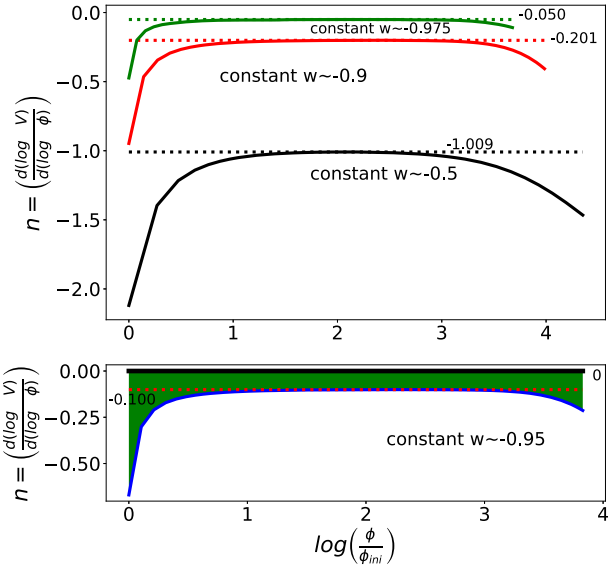

Figure 2. We plot the slope of the potential as a function of the field. From this log–log plot, we can see that there is an almost flat plateau with deviations at two ends. Thus the potential is close to a power law. In the upper panel, we plot three cases of constant w. The lower panel is for 3-σ constrained boundaries $(-1.0, -0.95)$ as described in the text. The shaded region is allowed a set of potentials as per the constraints found in Tripathi *et al.* (2017). The value of the constant central part changes with the value of constant w.

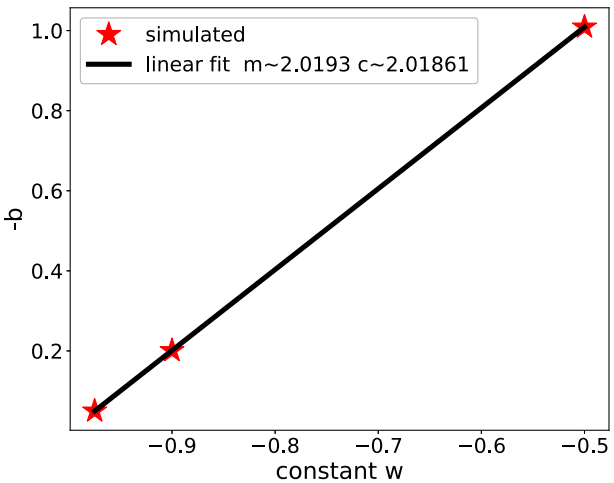

Figure 3. For different w = constant values, we obtain the approximate b for central linear part (as marked in Figure 2). As shown here, b values follow a linear relation with w. The fitted line has slope $m = 2.3163$ and intercept $c = 2.30258$.

study, Tripathi *et al.* (2017) combined the results from 3 different data sets to obtain 3σ confidence intervals for constant w and CPL $w(z)$ models. We use confidence intervals for the constant w while working in the regime $w \geq -1$, i.e., we use the confidence interval $(-1.0, -0.95)$ and reconstruct corresponding potential slope in the lower panel of Figure 2. This is shown as

a shaded region and marks the allowed slope for the potential. This is a simplistic approach and we are working on a detailed analysis while accounting for possible variations of other cosmological parameters.

2.3 *Quintessence*

The action for quintessence field is

$$I = \int d^4x\sqrt{-g}\left[\frac{1}{2}g^{\mu\nu}\partial_\mu\phi\partial_\nu\phi - V(\phi)\right], \tag{25}$$

with effective pressure and density

$$\rho_\phi = \frac{\dot{\phi}^2}{2} + V(\phi), \tag{26}$$

$$P_\phi = \frac{\dot{\phi}^2}{2} - V(\phi), \tag{27}$$

$$w_\phi = \frac{P_\phi}{\rho_\phi} = \frac{\dot{\phi}^2 - 2V}{\dot{\phi}^2 + 2V}. \tag{28}$$

For quintessence models of dark energy, w is related to time derivative of the field and the potential, and we have

$$\frac{\mathrm{d}\phi}{\mathrm{d}t} = \sqrt{(1+w)\rho_\phi} = \sqrt{(1+p+q(a-a_i))\rho_\phi}, \tag{29}$$

where

$$V(\phi) = \frac{1}{2}(1-w)\rho_\phi = \frac{1}{2}(1-p-q(a-a_i))\rho_\phi. \tag{30}$$

From Equations (3) and (29), we obtain

$$\frac{\mathrm{d}\phi}{\mathrm{d}t} = \sqrt{(1+p+q(a-a_i))\frac{3}{8\pi G}\frac{\beta}{a^{3(1+p-qa_i)}}\mathrm{e}^{-3q(a-a_i)}}. \tag{31}$$

Equation (31) can be combined with Equation (4) to obtain $\frac{\mathrm{d}\phi}{\mathrm{d}a}$. For potential, we have from Equations (30) and (3) as follows:

$$\frac{V}{H_i^2} = \frac{3}{2}\frac{(1-w)}{8\pi G}\frac{\beta}{a^{3(1+p-qa_i)}}\mathrm{e}^{-3q(a-a_i)}. \tag{32}$$

This system of equations specifies the solution.

2.4 *Quintessence field: Constant w*

For $w(a) =$ constant, we obtain a closed formula for $V(\phi)$ (see Sangwan *et al.* 2010 and references therein for previous work on this). In this case, Equation (31) reduces to

$$\frac{\mathrm{d}\phi}{\mathrm{d}t} = \sqrt{(1+w)\frac{3}{8\pi G}\frac{\beta}{a^{3(1+w)}}} \tag{33}$$

and

$$\frac{\mathrm{d}\phi}{\mathrm{d}a} = \sqrt{\frac{3(1+w)}{8\pi G}}\sqrt{\left[\frac{1}{\frac{\alpha a^{3w}}{\beta}+1}\right]}\left(\frac{1}{a}\right). \tag{34}$$

Defining

$$\lambda = \sqrt{\frac{3(1+w)}{8\pi G}} \tag{35}$$

and

$$x^2 = \frac{\alpha a^{3w}}{\beta} + 1, \tag{36}$$

we have

$$\phi(x) = C_1 + \frac{2\lambda}{3w}\int\frac{\mathrm{d}x}{x^2-1}. \tag{37}$$

Here C_1 is a constant of integration. The solution is

$$\phi(x) = -\frac{\lambda}{3w}[\log(1+x) - \log(x-1)]. \tag{38}$$

Inverting this, we get

$$x = \frac{\mathrm{e}^{-3w\phi/\lambda}+1}{\mathrm{e}^{-3w\phi/\lambda}-1}. \tag{39}$$

Defining

$$m = -\frac{3w\phi}{2\lambda}, \tag{40}$$

we rewrite Equation (39) as

$$x = \coth m \tag{41}$$

and we get

$$a^{3w} = \frac{\beta}{\alpha}[(\coth m)^2 - 1]. \tag{42}$$

Substituting this in Equation (32),

$$\frac{V(\phi)}{H_i^2} = \frac{3(1-w)\beta}{16\pi G}\left[\frac{\beta}{\alpha}((\coth m)^2-1)\right]^{-\frac{(1+w)}{w}}. \tag{43}$$

Equivalently,

$$\frac{V(\phi)}{H_i^2} = \frac{3(1-w)\beta}{16\pi G}\left[\frac{\alpha}{\beta}\sinh^2\left(-\frac{3w\phi\sqrt{8\pi G}}{2\sqrt{3(1+w)}}\right)\right]^{\frac{(1+w)}{w}}. \tag{44}$$

The derivations for constants w case for quintessence and phantom models were given by Sangwan *et al.* (2010) and they obtained the same form for quintessence models as in Equation (44). The reconstruction approach can be used to constrain potentials from observations, as was done in Sangwan *et al.* (2010). They used the

constrained ranges from Tripathi *et al.* (2017), to constrain the quintessence potentials for constant w. They also constrained the potentials for CPL and logarithmic $w(z)$ using some approximations. Their work can be numerically generalized, using formalism developed in this article, to various $w(z)$ for both tachyonic as well as quintessence models.

3. General case

For an arbitrary function $w(a)$, the continuity equation for that component is

$$\frac{\mathrm{d}\rho_\phi}{\rho} = -\frac{3(1+w)}{a}\mathrm{d}a \tag{45}$$

giving

$$\rho_\phi = \rho_{\phi_i} \exp\left[-3\int \frac{1+w}{a}\mathrm{d}a\right]. \tag{46}$$

Equivalently,

$$\Omega_\phi := \frac{8\pi G\rho_\phi}{3H_i^2} = \Omega_{\phi_i} \mathrm{e}^{-3\int \frac{1+w}{a}\mathrm{d}a}. \tag{47}$$

The subscript i represent values at some initial time.

Using this evolution equation for energy density, we can write differential equations for tachyon and quintessence fields:

$$\frac{\mathrm{d}\phi_{\mathrm{tach}}}{\mathrm{d}a} = \frac{\sqrt{1+w}}{\sqrt{\frac{\alpha}{a} + a^2\Omega_{\phi\mathrm{tach}}}}, \tag{48}$$

$$\frac{\mathrm{d}\phi_{\mathrm{q}}}{\mathrm{d}a} = \frac{\sqrt{3(1+w)\Omega_{\phi\mathrm{q}}}}{\sqrt{8\pi G}\sqrt{\frac{\alpha}{a} + a^2\Omega_{\phi\mathrm{q}}}}, \tag{49}$$

where $\Omega_{\phi\mathrm{q}}$ and $\Omega_{\phi\mathrm{tach}}$ are the quintessence and tachyon field density parameters scaled as shown in Equation (47) respectively. The potentials for the two fields are

$$\frac{V(a)}{H_i^2} = \frac{3(1-w)\Omega_{\phi\mathrm{q}}}{16\pi G}, \tag{50}$$

$$\frac{V(a)}{H_i^2} = \frac{3\sqrt{-w}\Omega_{\phi\mathrm{tach}}}{8\pi G}. \tag{51}$$

One can numerically integrate Equations (47) and (48)–(49) to get $\phi(a)$ and use (50)–(51) alongside to obtain $V(a)$. Hence one can obtain a numerical table of $V(\phi)$ vs. ϕ in the desired range. This table can be used for numerical fitting or interpolation functions. For example, cubic splines (Antia 2012) can be used for fitting to obtain spline coefficients which can be used for calculating $V(\phi)$ and its gradients, given a value of ϕ. Once we have spline coefficients and ϕ, the task is to find the interval in which the value of ϕ lies so that we can use coefficients corresponding to that interval. Evaluation of the function can be time consuming, but the fact that for background values ϕ there is a correspondence between ϕ and a, comes to our rescue. Typically perturbations have a small amplitude and hence deviation from background in a particular simulation domain is small, and this can be used to guess spline interval in that region. For example, one might be simulating a spherical collapse in a real space and perturbations may be really strong towards the centre, but they merge into the background as one moves away from the centre. In this case, for large radii, interval can be guessed from background and then one can move toward smaller radii. In this way, for each new inner point one has to only search in the adjacent intervals for interpolation if the field is continuous. As an example, we show here CPL potentials for quintessence and tachyon field in 4. The form obtained is similar to that obtained by Scherrer (2015).

4. Coupled quintessence mimicking ΛCDM

Minimally coupled quintessence models (Amendola 2000; Shahalam *et al.* 2015) can exactly mimic ΛCDM only with a completely flat potential, that is, no field dynamics is involved and the equations just reduce to that in case of Λ. However if energy exchange is allowed between quintessence field and dark matter, a Λ-like evolution is possible even with field dynamics and a time varying w. In this section, we consider a quintessence model with the following type of coupling (Barros *et al.* 2018):

$${}^{\phi}T^{\mu}_{\nu}{}_{,\mu} = Q\sqrt{8\pi G}\phi_{,\nu}\,\rho_{\mathrm{CDM}}, \tag{52}$$

$${}^{c}T^{\mu}_{\nu}{}_{,\mu} = -Q\sqrt{8\pi G}\phi_{,\nu}\,\rho_{\mathrm{CDM}}. \tag{53}$$

Please note a little different notation in this section, as described below. Q is the coupling constant between matter and quintessence. The subscript lCDM denotes the quantity corresponding to ΛCDM and the subscript 'CDM' is for the corresponding quantities for cold dark matter in the model with field, e.g. ρ_{CDM} is the density for cold dark matter in the model with an interacting dark energy field while $\rho_{l\mathrm{CDM}}$ is the cold dark matter density as evolved within ΛCDM. Also Ω_c^i is the density parameter for dark matter at initial time and Ω_Λ^i is Λ counterpart. The basic equations for this type of coupled model mimicking ΛCDM were derived in Barros *et al.* (2018). They wrote the potential $V(\phi)$ in terms of other variables, and did not specify exact formula for

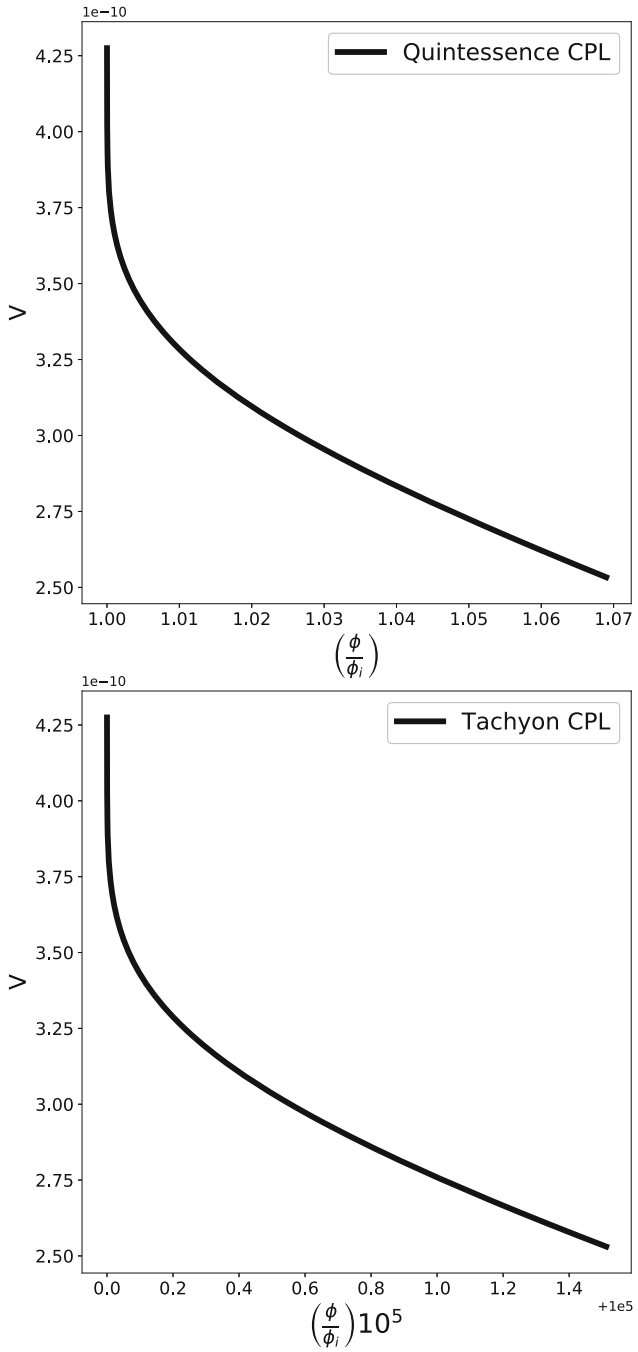

Figure 4. $V(\phi)$ simulated for CPL parametrization for quintessence and tachyon models. The shape of the curve is the same for quintessence and tachyon field but the rate of evolution of field is very different. The field traverses longer distances in field space for the quintessence case. This might have interesting implications in the context of Swampland criteria of string theory.

$V(\phi)$. Here we start from the equations derived in Barros *et al.* (2018) and then reconstruct the formula for potential that gives the required Λ-like behaviour. For a field model giving the same $a(t)$ as that of ΛCDM, we have

$$\left(\frac{\dot{a}}{a}\right) = \left(\frac{\dot{a}}{a}\right)_{\Lambda\text{CDM}}. \tag{54}$$

Ignoring baryons and radiation, we have

$$\rho_{\text{CDM}} + \rho_\phi = \rho_{l\text{CDM}} + \rho_\Lambda \tag{55}$$

and

$$p_\phi = p_\Lambda = -\rho_\Lambda. \tag{56}$$

Combining the two, we have

$$\dot{\phi}^2 = \rho_{l\text{CDM}-\rho\text{CDM}}. \tag{57}$$

The continuity equation for matter is

$$\dot{\rho}_{\text{CDM}} + 3H\rho_{\text{CDM}} = -Q\sqrt{8\pi G}\dot{\phi}\rho_{\text{CDM}}, \tag{58}$$

giving

$$\rho_{\text{CDM}} = \rho^i_{\text{CDM}}\frac{a_i^3}{a^3}e^{-Q\sqrt{8\pi G}\phi}. \tag{59}$$

Using (57) and (59) along with the standard Friedmann equation for ΛCDM, we get

$$\frac{d\phi}{da} = \sqrt{\left(\frac{3}{8\pi G}\right)}\left(\frac{1}{a}\right)\frac{\sqrt{1-e^{-Q\sqrt{8\pi G}\phi}}}{\sqrt{1+\frac{\Omega^i_\Lambda a^3}{\Omega^i_c a_i^3}}}. \tag{60}$$

Arranging and integrating the equation, we obtain

$$\begin{aligned}\omega \quad &\log\left[\sqrt{e^{Q\sqrt{8\pi G}\phi}-1}+e^{Q\sqrt{8\pi G}\phi/2}\right] \\ &= \log\left[\frac{\sqrt{1+\frac{\Omega^i_\Lambda a^3}{\Omega^i_c a_i^3}}-1}{\sqrt{1+\frac{\Omega^i_\Lambda a^3}{\Omega^i_c a_i^3}}+1}\right],\end{aligned} \tag{61}$$

where $\omega = \pm\frac{2\sqrt{3}}{Q}$ ($-$ for negative Q). Writing $a(\phi)$ as a function of ϕ, we have

$$a^3(\phi) = \frac{4C_1\Omega^i_c a_i^3}{\Omega^i_\Lambda}\left[\frac{f(\phi)^\omega}{(1-C_1 f(\phi)^\omega)^2}\right] \tag{62}$$

with C_1 taking care of any constant of integration and

$$f(\phi) = \sqrt{e^{Q\sqrt{8\pi G}\phi}-1}+e^{Q\sqrt{8\pi G}\phi/2}. \tag{63}$$

The potential V can be obtained from Equations (56), (57) and (59) as

$$\frac{V(\phi)}{H_i^2} = \frac{3\Omega^i_c}{8\pi G}\left[\frac{a_i^3}{2(a^3(\phi))}(1-e^{-Q\sqrt{8\pi G}\phi})+\frac{\Omega^i_\Lambda}{\Omega^i_c}\right], \tag{64}$$

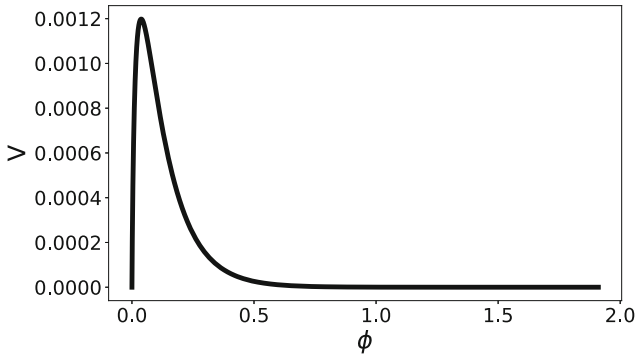

Figure 5. $V(\phi)$ for coupled quintessence mimicking ΛCDM in background kinematics.

where $a^3(\phi)$ has a functional form as mentioned in (62). The form of the potential is illustrated in Figure 5.

$$V_{,\phi} = \frac{3\Omega_c^i}{8\pi G}\left[\frac{Q\sqrt{8\pi G}\mathrm{e}^{-Q\sqrt{8\pi G}\phi}a_i^3}{2a^3} - \frac{a_i^3}{2a^6}\frac{\mathrm{d}(a^3)}{\mathrm{d}f}\frac{\mathrm{d}f}{\mathrm{d}\phi}(1-\mathrm{e}^{-Q\sqrt{8\pi G}\phi})\right]. \quad (65)$$

Studies of perturbations in the coupled quintessence models play an important role in distinguishing these from ΛCDM models. Our analysis of such models will be reported elsewhere.

5. Summary

In this work, we have described basic equations for reconstructing potentials for quintessence and tachyon field. We have given results for the w = constant case. We show that analytical closed formulas are possible for quintessence potentials in these cases while for tachyon fields, such formulae are obtained only for the $w = -0.5$ case. For other values of constant w, we provide formulae for numerical reconstruction. We also find a rough approximation to these constant w potentials for tachyon dark energy. We describe numerical methods for numerical construction of tachyon and quintessence potentials for arbitrary $w(a)$. From numerical calculation of potentials for CPL cases for quintessence and tachyon, we show that the shape of the potential is the same for both of these, but the field rolls much more in quintessence case than in the tachyon case. This could motivate further investigations in the context of string Swampland (Heisenberg *et al.* 2018; Agrawal *et al.* 2018; Akrami *et al.* 2019). We have also studied coupled quintessence models.

The results of this study can be used for analysis of perturbations in such models. In particular, we can compare growth of perturbations in models of different types that have the same expansion history. We will report results on spherical collapse in perturbed dark energy models in a forthcoming publication.

Acknowledgements

The authors thank Dr. Ankan Mukherjee, Dr. H. K. Jassal, Dr. Varadharaj Srinivasan and Avinash Singh for useful discussions. This research has made use of NASA's Astrophysics Data System Bibliographic Services.

References

Agrawal P., Obied G., Steinhardt P. J., Vafa C. 2018, Phys. Lett. B, 784, 271, https://doi.org/10.1016/j.physletb.2018.07.040. arXiv:1806.09718 [hep-th]

Akrami Y., Kallosh R., Linde A., Vardanyan V. 2019, Fortsch. Phys., 67(1-2), 1800075, https://doi.org/10.1002/prop.201800075. arXiv:1808.09440 [hep-th]

Amendola L. 2000, Phys. Rev. D, 62, 043511, https://doi.org/10.1103/PhysRevD.62.043511. arXiv:astro-ph/9908023

Amendola L., Tsujikawa S. 2010, Dark Energy: Theory and Observations, Cambridge University Press, Cambridge

Antia H. 2012, Numerical Methods for Scientists and Engineers, Hindustan Book Agency, New Delhi

Bagla J. S., Padmanabhan T., Narlikar J. V. 1996, Commun. Astrophys., 18, 275

Bagla J. S., Jassal H. K., Padmanabhan T. 2003, Phys. Rev. D, 67, 063504

Bamba K., Capozziello S., Nojiri S., Odintsov S. D. 2012, Astrophys. Space Sci., 342, 155, https://doi.org/10.1007/s10509-012-1181-8. arXiv:1205.3421 [gr-qc]

Barros B. J., Amendola L., Barreiro T., Nunes N. J. 2018, Coupled quintessence with a ΛCDM background: Removing the σ_8 tension, arXiv e-prints, February 2018

Battye R. A., Pace F. 2016, Phys. Rev. D, 94(6), 063513, https://doi.org/10.1103/PhysRevD.94.063513. arXiv:1607.01720 [astro-ph.CO]

Caldwell R. R., Dave R., Steinhardt P. J. 1998, Phys. Rev. Lett., 80, 1582

Chevallier M., Polarski D. 2001, Int. J. Mod. Phys. D, 10, 213, https://doi.org/10.1142/S0218271801000822. arXiv:gr-qc/0009008

Clarkson C., Zunckel C. 2010, Phys. Rev. Lett., 104, 211301, https://doi.org/10.1103/PhysRevLett.104.211301. arXiv:1002.5004 [astro-ph.CO]

De Bernardis F., Martinelli M., Melchiorri A., Mena O., Cooray A. 2011, Phys. Rev. D, 84, 023504, https://doi.org/

10.1103/PhysRevD.84.023504. arXiv:1104.0652 [astro-ph.CO]
Durrer R. 2011, Philos. Trans. R. Soc. A, 369. http://doi.org/10.1098/rsta.2011.0285
Efstathiou G., Sutherland W. J., Maddox S. J. 1990, *Nature*, 348, 705
Gerke B. F., Efstathiou G. 2002, Mon. Not. R. Astron. Soc., 335(1), 33
Heisenberg L., Bartelmann M., Brandenberger R., Refregier A. 2018, Phys. Rev. D, 98(12), 123502, https://doi.org/10.1103/PhysRevD.98.123502. arXiv:1808.02877 [astro-ph.CO]
Huterer D., Turner M. S. 1999, PRD, 60, 081301
Huterer D., Shafer D. L. 2018, Rep. Prog. Phys., 81(1), 016901, https://doi.org/10.1088/1361-6633/aa997e. arXiv:1709.01091 [astro-ph.CO]
Jassal H. K. 2012, Phys. Rev. D, 86, 043528, https://doi.org/10.1103/PhysRevD.86.043528. arXiv:1203.5171 [astro-ph.CO]
Li C., Holz D. E., Cooray A. 2007, PRD, 75, 103503
Linder E. V. 2003, Phys. Rev. Lett., 90, 091301, https://doi.org/10.1103/PhysRevLett.90.091301. arXiv:astro-ph/0208512
Mifsud J., Van De Bruck C. 2017, JCAP, 1711(11), 001, https://doi.org/10.1088/1475-7516/2017/11/001. arXiv:1707.07667 [astro-ph.CO]
Ostriker J. P., Steinhardt P. J. 1995, Nature, 377, 600
Padmanabhan T. 2002, Phys. Rev. D,, 66(2), 021301
Pearson J. W. 2009, Computation of hypergeometric functions, Ph.D. thesis, 2009
Perlmutter S., Aldering G., Goldhaber G. *et al.* 1999, ApJ, 517, 565
Pettorino V., Baccigalupi C. 2008, Phys. Rev. D, 77, 103003, https://doi.org/10.1103/PhysRevD.77.103003. arXiv:0802.1086 [astro-ph]
Rajvanshi M. P., Bagla J. S. 2018, JCAP, 1806(06), 018, https://doi.org/10.1088/1475-7516/2018/06/018. arXiv:1802.05840 [astro-ph.CO]
Riess A. G., Filippenko A. V., Challis P. *et al.* 1998, AJ, 116, 1009
Sahni V., Starobinsky A. 2006, Int. J. Mod. Phys. D, 15, 2105, https://doi.org/10.1142/S0218271806009704. arXiv:astro-ph/0610026
Saini T. D., Raychaudhury S., Sahni V., Starobinsky A. A. 2000, Phys. Rev. Lett., 85, 1162, https://doi.org/10.1103/PhysRevLett.85.1162. arXiv:astro-ph/9910231
Sangwan A., Mukherjee A., Jassal H. K. 2010, JCAP, 1, 018
Scherrer R. J. 2015, Phys. Rev. D, 92(4), 043001 https://doi.org/10.1103/PhysRevD.92.043001. arXiv:1505.05781 [astro-ph.CO]
Shahalam M., Pathak S. D., Verma M. M., Khlopov M. Y., Myrzakulov R. 2015, Eur. Phys. J. C, 75(8), 395, https://doi.org/10.1140/epjc/s10052-015-3608-1. arXiv:1503.08712 [gr-qc]
Tripathi A., Sangwan A., Jassal H. K. 2017, JCAP, 1706(06), 012, https://doi.org/10.1088/1475-7516/2017/06/012. arXiv:1611.01899 [astro-ph.CO]
Tsujikawa S. 2013, Class. Quantum Gravit., 30(21), 214003
Wang Y. T., Xu L. X., Gui Y. X. 2010, Phys. Rev. D, 82, 083522, https://doi.org/10.1103/PhysRevD.82.083522
Weisstein E. W. 2018, Incomplete beta function, from mathworld—a wolfram web resource. http://mathworld.wolfram.com/IncompleteBetaFunction.html, accessed: 2018-10-15
Wu P., Yu H. W. 2007, JCAP, 0710, 014, https://doi.org/10.1088/1475-7516/2007/10/014. arXiv:0710.1958 [astro-ph]
Yang W., Li H., Wu Y., Lu J. 2016, JCAP, 1610(10), 007, https://doi.org/10.1088/1475-7516/2016/10/007. arXiv:1608.07039 [astro-ph.CO]